Iodine Sequestration by Thiol-Modified MIL-53(Al)

Alexis S. Munn,[1] Franck Millange,[2] Michel Frigoli,[3] Nathalie Guillou,[3] Clément Falaise,[4] Victoria Stevenson,[4] Christophe Volkringer,[4,5] Thierry Loiseau,[4] Giannantonio Cibin,[6] and Richard I. Walton[1,*]

1. Department of Chemistry, University of Warwick, Coventry, CV4 7AL, U.K.

Email: r.i.walton@ warwick.ac.uk

2. Département de Chimie, Université de Versailles-St-Quentin-en-Yvelines, Université Paris-Saclay, 45 Avenue des États-Unis, 78035 Versailles cedex, France.

3. Institut Lavoisier Versailles, UMR CNRS 8180, Université de Versailles St-Quentin-en-Yvelines, Université Paris-Saclay, 45 Avenue des États-Unis, 78035 Versailles cedex, France.

4. Unité de Catalyse et Chimie du Solide (UCCS) - UMR CNRS 8181, Université de Lille Nord de France, USTL-ENSCL, Bat C7, BP 90108, 59652 Villeneuve d'Ascq, France.

5. Institut Universitaire de France, 1 rue Descartes, 75231 Paris Cedex 05, France.

6. Diamond Light Source Ltd., Harwell Science and Innovation Campus, Didcot OX11 0DE, U.K.

Abstract

A thiol-modified version of the porous metal organic framework MIL-53 is synthesised in a single step using the functionalised ligand precursor 2,5-dithiol-1,4-benzenedicarboxylic acid and aluminium as the framework metal. Careful washing is needed to remove unreacted and dimerised linker from the material after synthesis, but once performed profile fitting of powder X-ray diffraction shows that thiol-modified MIL-53(Al) presents a closed, narrow-pore, structure with unit cell volume ~1103 Å^3 (space group *C*2/*c*). The presence of intact thiol groups is confirmed using sulfur K-edge XANES spectroscopy and IR spectroscopy, while nitrogen BET surface area analysis and krypton and xenon adsorption isotherms reveal the porosity of the material. The thiol-modified solid is capable of iodine adsorption from the vapour phase and from solution and

an equilibrium uptake of ~325 mg per g is reached, which is higher than other reported modified forms of MIL-53. Infrared spectroscopy shows the disappearance of the S-H stretch after iodine adsorption, while sulfur K-edge XANES shows a complex spectrum, consistent with the formation of sulfenyl iodide but also oxidation of some sulfur to disulfide having occurred. We therefore propose that formation of covalent S-I bonds allows the sequestration of iodine by the porous solid, but that a proportion of the thiol groups are also in close enough proximity for the formation of disulfide links.

Introduction

Porous materials with the MIL-53 structure are the most studied flexible metal-organic frameworks (MOFs). These materials have ideal composition M(BDC)(OH), where M is a trivalent metal, such as Al, Cr, Fe, Ga, Sc, and BDC is 1,4-benzenedicarboxylate (terephthalate).[1] The metal centres are octahedrally coordinated by four oxygen donors of the organic linkers and two *trans* hydroxide ions that form a backbone of an inorganic chain of corner-shared octahedra. The chains are cross-linked by the bridging BDC linkers to generate diamond-shaped channels that run parallel to the chains. The structural flexibility of MIL-53 materials arises from changes in the dihedral angles defining the connections of the carboxylates and pairs of metals, such that a massive volume expansion of up to 80 % can be brought about by an external stimulus such as temperature, pressure, or by changing the guest molecules present in the porous structure, see Figures 1a-d.[2] One of the simplest modifications of the MIL-53 structure is replacement of some of the hydroxide by fluoride (during synthesis of the material) and this can modify the structural flexibility.[3] Likewise, partial replacement of one trivalent metal by another can adjust the response of the framework to stimuli.[4] The potentially most versatile method of modification of MIL-53 materials, however, is the addition of functional groups to the aromatic ring of the terephthalate linker: this has been widely studied for a range of substituents and a common strategy is to pre-make substituted 1,4-benzenedicarboxylic acid that is then used as a reagent for the crystallisation of MIL-53.[5, 6] This has been used with great effect to modify the response of the

MIL-53 towards guest molecules and their thermally induced breathing behaviour,[7, 8, 9] or to introduce reactive functionalities that can be used for further chemical modification.[10]

Thiol-modified MOFs have been reported, where the organic linker contains R-SH moieties. Yee *et al.* used 2,5-dithiol-1,4-benzenedicarboxylic acid as a linker precursor for the formation of the Zr MOF UiO-66 and the Al MOF CAU-1 and showed how the resulting solids could be used as effective mercury adsorbents, either Hg^{2+} from solution or Hg vapour.[11] The same group later showed that a Hg^{2+} loaded thiol-modified MOF could be oxidised using H_2O_2 to produce an effective catalyst for room temperature acetylene hydrogenation,[12] while Gui *et al.* prepared a Zr MOF from thiol-modified linkers and anchored Pd(II) for catalysis.[13] Burrows *et al.* formed Zn MOFs with reactive thioether functionalised ligands that could be used for further post-synthesis modification.[14] Thiophene-based ligands can also be included in MOF structures and used to extract selectively Cu^{2+} from other divalent metals,[15] and in related work, thio-ether containing linkers have been incorporated into the prototypical material MOF-5 to produce a solid with nitrobenzene sensing properties and a sensitivity towards small amounts of $HgCl_2$ in solution.[16] Zhou *et al.* used the linker tetrakis(methylthio)benzenedicarboxylate to form a Pb^{2+} network with pendant methylthio- groups that could adsorb $HgCl_2$,[17] and also for a mixed valent Cu^{+}/Cu^{2+} network that could adsorb ammonia and amines.[18] Ke *et al.* introduced dithiols into HKUST-1, which contains coordinatively unsaturated Cu(II) centres, post-synthesis and used the pendant thiols as centres for effective Hg^{2+} adsorption from solution.[19] Others have shown that post-synthetic modification allows thiol groups to be added to a pre-made MOF: in the case of MIL-101(Cr) this allowed formation of an Hg^{2+} adsorbent.[20]

In this paper we explore the possibility of producing a thiol-modified MIL-53, and use, for the first time, sulfur K-edge XANES spectroscopy to prove successful incorporation of a thiolated ligand into a MOF. To our knowledge the only previous attempt to add thiol groups to MIL-53 used post-synthetic reaction of amino-modified MIL-53 with mercaptoacetic acid.[21] Herein we use 2,5-dithiol-1,4-benzenedicarboxylic acid, Figure 2b, as a linker precursor to form thiol-modified MIL-53(Al) and test the resulting solid for adsorbing iodine. Adsorption of iodine is of relevance for decontamination of nuclear by-products formed during the fission of uranium and plutonium:

the beta emitter ^{129}I has a half-life of 15.7 million years and while other radioactive isotopes have much shorter half-lives, the volatility of iodine and its role in human metabolic processes mean that materials for its capture are highly sought after.[22]

Experimental

Synthesis of the linker precursor 2,5-dithiol-1,4-benzenedicarboxylic acid (2,5-dimercaptoterephthalic acid) was performed according to the method of Vial *et al.*[23] The quantities of reactants for each step were adjusted in order to obtain ~10 g of the 2,5-dithiol-1,4-benzenedicarboxylic acid. ^{1}H NMR (300 MHz, DMSO): δ 8.33 (s, 2H, CHAr) (see ESI).

To prepare MIL-53 materials, $Al(ClO_4)_3 \cdot 9H_2O$ (1.96 g, 4.02 mmol), 2,5-dithiol-1,4-benzenedicarboxylic acid (0.47 g, 4.02 mmol) and 10 mL *N*,*N*-diethylformamide were combined in a 20 mL Teflon-lined autoclave, stirred for 15 minutes and then heated to 125 °C for 5 hrs. The resulting yellow powder was stirred in a large amount of methanol for 1-5 days and the suspension was then centrifuged to collect. The sample was separated as product **A** and **B** after a colour change was observed during the washing procedure; product **B** is a slightly darker shade of pale yellow. Product **A** was isolated after stirring for 1-3 days in methanol and product **B** was produced after stirring for 4-5 days. Both samples were dried in air at approximately 70 °C. The combination of aluminium perchlorate as the Al reagent and *N*,*N*-diethylformamide as solvent was selected as preliminary experiments found this provided the shortest reaction time to prevent ligand decomposition.

Powder X-ray diffraction data were recorded from finely ground samples performed using either a Siemens D5000 diffractometer operating with Cu $K\alpha_{1/2}$ radiations ($\lambda_{average}$ = 1.5418 Å) or a Panalytical X'Pert Pro MPD operating with Cu $K\alpha_1$ radiation ($\lambda_{K\alpha1}$ = 1.5406 Å). Extractions from the peak positions, pattern indexing, and whole powder pattern fitting without reference to a structural model were carried out with the TOPAS program.[24]

Sulfur K-edge XANES (X-ray absorption near edge structure) spectroscopy was performed on the B18 beamline at Diamond Light Source, UK. Data were measured in total

electron yield (TEY) from powdered samples deposited on conducting adhesive graphite tape in a helium filled chamber. Beam intensity on the sample was monitored using a helium-filled ion chamber, and a Si(III) double-crystal monochromator was used to select the incident energy, while Cr-coated mirrors were used to collimate the beam before the monochromator and to focus on the sample position. The beam size on the sample was estimated to be 1 x 1 mm^2. TEY signal was collected from the sample holder drain current with a polarisation of 30 V cm^{-1} applied. Spectra were recorded with step-size of 0.2 eV in quick-EXAFS mode with 5 minutes per scan and 3 repetitions. Data analysis was performed using the Athena software[25] with XANES spectra produced by normalisation to the edge step after subtraction of pre-edge and post-edge backgrounds.

Thermogravimetric analysis (TGA) was performed using a Mettler Toledo Systems TGA/DSC 1 instrument under an air flow of 50 ml min^{-1} from room temperature to 1000 °C at a heating rate of 10 °C min^{-1}. Elemental analysis for C,H,N and S was performed by Medac Ltd, UK. Raman spectra were recorded from solid samples using a Bruker MultiRAM spectrometer operating with a Nd:YAG laser (1064 nm) with 4 cm^{-1} resolution and either 50 mW or 200 mW incident beam depending on the stability of the sample to the laser.

All the gas sorption measurements were performed using a Micromeritics ASAP 2020 apparatus. Before gas sorption the material was activated at 200°C under vacuum. The porosity of the sample was estimated by gas sorption isotherm experiment in liquid nitrogen (77 K). For surface area calculation, BET and Langmuir surface areas were determined from 0.01-0.2 and 0.06-0.2 p/p_0 ranges, respectively. The calculation of micropore volume is based on t-plot method, in the 0.09-0.7 p/p_0 range. Kr and Xe experiments were realised at 273.15 K, up to 900 mmHg.

IR spectra were recorded at room temperature using a Bruker ALPHA FTIR spectrometer with a Diamond attenuated total reflection attachment. Measurements were performed on solid powder samples with 8 scans recorded, along with an air background measurement.

For iodine kinetic adsorption, the activated material (30 mg) was stored in a cell under continuous flow of gaseous iodine (0.87 mg of I_2 per hour, argon as carrier gas), generated by a permeation oven (Vinci Dynacalibrator Model). The quantity of iodine trapped within the MOF was determined by UV/vis spectroscopy (scan every 4 minutes), by dosing the remaining iodine concentration which was not adsorbed by the MOF compound. The difference between the quantity delivered by the permeation oven and the quantity not trapped by the MOF leads to the plot of a kinetic curve.

Results and Discussion

Powder XRD shows that the lighter coloured product of the solvothermal reaction Product **A** has a pattern characteristic of the fully expanded form of MIL-53 and resembles to the MIL-53(Al) prepared with dihydroxo-substituted linker (MIL-53(Al)-$(OH)_2$, unit cell volume = 1410.4(28) Å^3).[6] Therefore, the unit cell parameters, previously determined for as-made MIL-53(Al)-$(OH)_2$, were used directly for the whole powder pattern fitting (Figure 2a). The majority of the observed peaks can be indexed in an orthorhombic unit cell (space group *Imcm*) *a* = 17.32(5) Å *b* = 12.05(2) Å *c* = 6.70(2) Å, and with a volume of 1398(6) Å^3, which is in good agreement with the presence of the large pore form of MIL-53,[1] as indicated on Figure 1c. It should be noted that the powder diffraction line observed at about 10.8° corresponds to a very small amount of Product **B**. Product **B** presents a closed structure, *i.e.* the narrow pore form of the MIL-53 structure,[1] as shown on Figure 1a, albeit with a trace of the open form remaining. The powder pattern could be indexed after eliminating the two major peaks of the Product **A**. Two candidate unit cells with similar unit cell volume (~1100 Å^3) and figure of merits could be obtained by the indexing LSI method in the orthorhombic and monoclinic systems. Taking into account the broad peak widths, it was impossible to choose between these two cells. However, most of the MIL-53(Al) materials with a unit cell volume close to 1100 Å^3 have been previously indexed in a monoclinic unit cell.[8] Based on this knowledge, this lead us to choose the *C*2/*c* space group and the refined lattice parameter (*a* = 19.89(2) Å *b* = 8.732(3) Å *c* = 6.699(4) Å β

= 108.6(1)° and V =1103(1) Å^3) were determined after pattern matching (Figure 1b). These compare well with the MIL-53(Al) with bromo-substituted linker, which has been reported with cell volume ~ 1055 Å^3 (*a* = 19.567(14), *b* = 8.532(12) *c* = 6.616(5) β = 107.22(6)°).[6] It should be noted that in both cases (Products **A** and **B**), the *c* parameter was restrained to vary from 6.6 to 6.7 Å, as expected for the MIL-53(Al) structure, in order to obtain consistent results regarding the expected geometry of the Al-OH-Al chains. The powder XRD patterns show considerable peak broadening, suggesting either small crystallites or microstrain due to some inherent disorder in the structure (such as static disordered of ligand substituent positions), but this is typical for linker-modified MIL-53 materials for which full structure refinement has rarely been proved possible.[9]

The incorporation of the intact ligand was confirmed by sulfur K-edge XANES spectroscopy, Figure 3. As shown by Vairavamurthy, the position of the sulfur K-edge XANES signal is diagnostic of the chemical environment and oxidation state of sulfur in both inorganic solids and organic molecules,[26] with the edge position of thiols is shifted by ~ 1 eV to higher energy than elemental sulfur, while disulfides show a much smaller shift. For our materials, we compared the sulfur K-edge XANES signal with pristine linker: this shows that for Product **B** the sulfur is largely present in the same environment as the linker itself, while for Product **A**, the edge shift and difference in post-edge region is indicative of the presence of disulfide links.

TGA, Figure 4, shows that Product **A** has additional mass loss at less than 200 °C compared to Product **B**, which would suggest excess unreacted linker or excess solvent in the first sample. Elemental analysis gives a consistent picture with good agreement for Product **B** with the expected empirical formula $Al(C_8H_4O_4S_2)(OH)\cdot[H_2O]$: observed 31.78 % C, 2.28 % H, 20.05 % S, expected 33.10 % C, 2.08 % H, 22.09 % S. Thus, we propose that Product **A** contains excess linker that has dimerised and/or decomposed into some disulfide-containing species (as seen by XANES), while more careful washing leads to Product **B** that is the dithiol modified MIL-53. Therefore, our remaining analysis is focussed on Product **B**. The slightly high sulfur content of even this material suggests that there may be a small amount of disulfide that cannot be

removed by washing. This is consistent with the XANES spectroscopy as the edge position of Product **B** is shifted to slightly lower energy than the pristine linker, Figure 3.

The BET surface area measured using nitrogen porosimetry on a sample degassed by heating in vacuum at 200 ^{o}C was measured as 324 m^2g^{-1} with micropore volume = 0.07 cm^3g^{-1} for the activated compound and Langmuir surface area = 384 m^2g^{-1}. The BET surface area value is noticeably lower than for MIL-53(Al) in its unmodified form, for which values in excess of 1100 m^2g^{-1} are typically reported (micropore volume of 0.5 cm^3g^{-1}),[27] but this behaviour is similar to that seen in the other forms of MIL-53 with modified linkers, such as the case of dihydroxy- or bromo-, where a very small nitrogen uptake was ascribed to the bulky substituents.[6] Thus for the dithiolated material we conclude the material exists in a closed structure and presents a non-breathing framework.

By analogy with previous studies dedicated to the sorption of xenon in unmodified MIL-53(Al),[28] the narrow pore form of the thiol-modified framework is also confirmed by the low uptake (28 cm^3 g^{-1} at 900 mmHg) of xenon at 273.15K (Figure 5). Due to the difference in polarisability between Xe and Kr,[29] the adsorption of Kr leads to a smaller quantity of Kr trapped within the framework (16 $cm^3.g^{-1}$ at 900 mmHg) at the same temperature (Figure 5).

Iodine uptake, Figure 6, shows a steep uptake in 12 hours to give more than 90 % of final value, with maximum uptake of ~325 mg per g of MOF reached after > 2 days. This value is higher than for MIL-53(Al)-NH_2, in the case of capture of iodine from cyclohexane solution.[30] However, this uptake remains lower than those calculated for other recently reported sorbents based on sulfur-containing functionalities such as polysulfide LDHs (1.3 to 1.5 g/g)[31] or chalcogenide aerogels (2.2 g/g).[32]

IR spectroscopy was used to verify the loss of S-H groups after addition of iodine on Product **B**, Figure 7a. This shows the disappearance of the characteristic S-H stretching vibration at 2560 cm^{-1} after interaction with iodine. Importantly, this also shows that the framework of the MIL-53 remains intact after iodine modification, since all bands due to the 1,4-benzenedicarboxylate moieties are unchanged. After exposure to iodine, whether in the vapour phase or from solution, crystallinity of the solids is reduced, but diffraction features are seen at

low angle that are characteristic of the open form of MIL-53 and the relative weak intensity of the low angle features compared to those at higher angles is indicative of pore filling by electron-rich iodide species (see ESI). Furthermore, thermogravimetric analysis of the solids after iodine addition (either from solution or from the vapour phase) shows an additional mass loss at 200-300 °C that can be ascribed to loss of iodine (see ESI).

The interaction of iodine with a thiol-modified MOF has recently been investigated by Yee *et al.* who described the synthesis of the Zr MOF UiO-66 with and showed reaction with iodine gave sulfenyl iodide (S-I) units in the structure, with HI as the second product.[33] Although they did not quantify uptake iodine with time, it was proposed that iodine can be sequestered effectively by formation of covalent S-I bond. Our material shows a distinct darkening in colour after iodine addition (see Supporting Information), which is comparable to that reported for the UiO-66 MOF.[33] To investigate further the possibility of sulfenyl iodide formation we performed S K-edge XANES experiments on a sample after exposure to iodine in solution to reach equilibration (1 M solution in chloroform solution at room temperature for 3 days), Figure 7b. These spectra show that after reaction with iodine there are at least two distinct chemical environments for sulfur. First, there is evidence for oxidation of some of the thiol groups to disulfide, with a shift of part of the spectrum to lower energy (*cf.* the spectrum from incompletely washed Product **A** in Figure 3), consistent with the 'oxidation level' calibration scale proposed by Vairavamurthy.[26] The remainder of the sulfur shows a spectrum shifted to higher energy than the pristine material, which is consistent with a portion of the sulfur being covalently bonded to the more electronegative iodine. This supports the proposition of the formation of sulfenyl iodide groups. The measured saturation uptake of iodine of 325 mg/g of material corresponds to close to 1 mole of iodine atoms per 3 of sulfur atoms in the solid (assuming the chemical formula based on the elemental analysis above). Thus approximately 30 % of the S-H groups have reacted with iodine to form S-I. This is consistent with some of the sulfur being converted to disulfide by the action of iodine, implying that some of the thiol functionalities are in close enough proximity to interact. Of the remaining sulfur much of this is converted to sulfenyl iodide groups, giving the

dark colour of the iodine-adsorbed solid. Further evidence for the formation of sulfenyl iodide comes from Raman spectroscopy (ESI): the formation of a band at around 360 cm^{-1} implies the presence of S-I bonds. [33] This band is rather weaker than seen by Yee *et al.* in their UiO-66 material, which is not unexpected due to the low crystallinity of our materials. We also note that Raman shows the removal of S-H upon reaction with iodine and an increase amount of S-S bonding, consistent with the idea of formation of some disulfide by oxidation of a proportion of the thiol groups.

Conclusions

We have shown how a thiol modified form of the prototypical flexible metal-organic framework MIL-53 allows capture of iodine, which is relevant for clean-up of radioactive nuclear by-products. While there is some evidence for the formation of disulfide by the action of iodine, the formation of a covalent S-I bond is proposed as the mechanism of adsorption, which is distinct from other proposed iodine adsorbents, such as those with amine or polysulfide functionalities. The work points towards using MOFs with greater porosity for thiol modification to increase the capacity of iodine in the solid state by making more of the thiol functionalities accessible and also minimising their interaction with each other to avoid disulfide formation. Finally we note that while sequestration of iodine does not necessarily require recycling of the host, it may be possible to release the iodine by use of 1,2-ethanedithiol as shown by Yee *et al.* in their thiol modified UiO-66 MOF,[33] while the TGA data suggest a thermal release may also be possible.

Acknowledgments

ASM and RIW acknowledge the financial support of the European Community (FP7/2007-2013, grant agreement 228862) and are grateful to Diamond Light Source Ltd for provision of beamtime. CV and TL thank the French National Research Agency (ANR) which funded a part of this work, through the PIA (Programme d'Investissement d'Avenir) under contract "ANR-11-RSNR-0013-01" (Mire project: Mitigation of outside releases in case of nuclear accident). We thank James Crosland for measuring IR spectra.

Figures

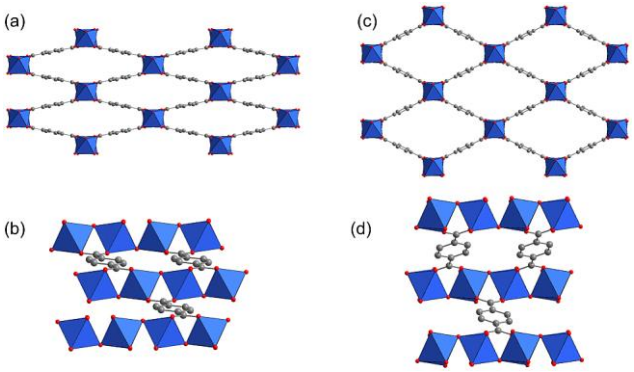

Figure 1: Structural views of the (a) and (b) closed (narrow pore) and (c) and (d) open (large pore) forms of the MIL-53 structure, with metal-centred octahedral shown in blue and the carbons of the 1,4-benzenedicarboxylate linker in grey. No guest molecules are shown.

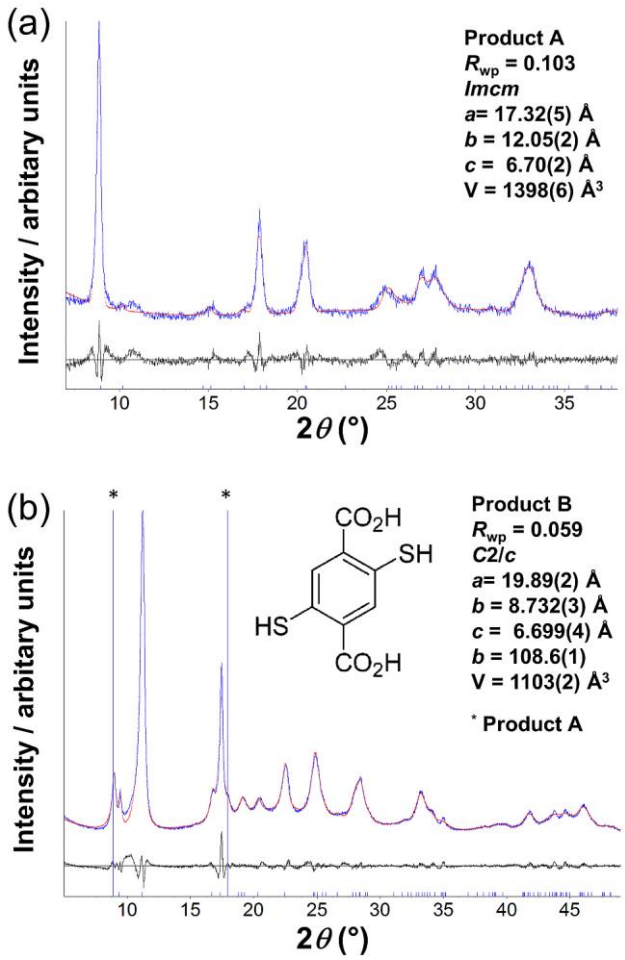

Figure 2: Powder XRD profile fits (a) for Product **A** (λ = 1.5418 Å) and (b) for Product B (λ = 1.5406 Å)**.** The blue line is the measured data, the red line the fitted curve and the black line the difference. The blue tick marks on the *x*-axes represent the positions of allowed Bragg reflections. In (b) the molecular formula of the ligand precursor 2,5-dithiol-1,4-benzenedicarboxylic acid is shown.

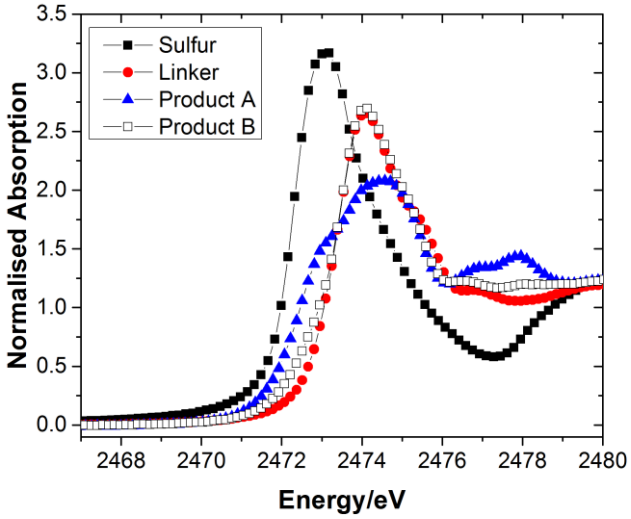

Figure 3: S K-edge XANES spectra of the thiol-modified MIL-53 materials (Product **A** and Product **B**), elemental α-sulfur and the pristine linker precursor (2,5-dithiol-1,4-benzenedicarboxylic aid) as reference compounds.

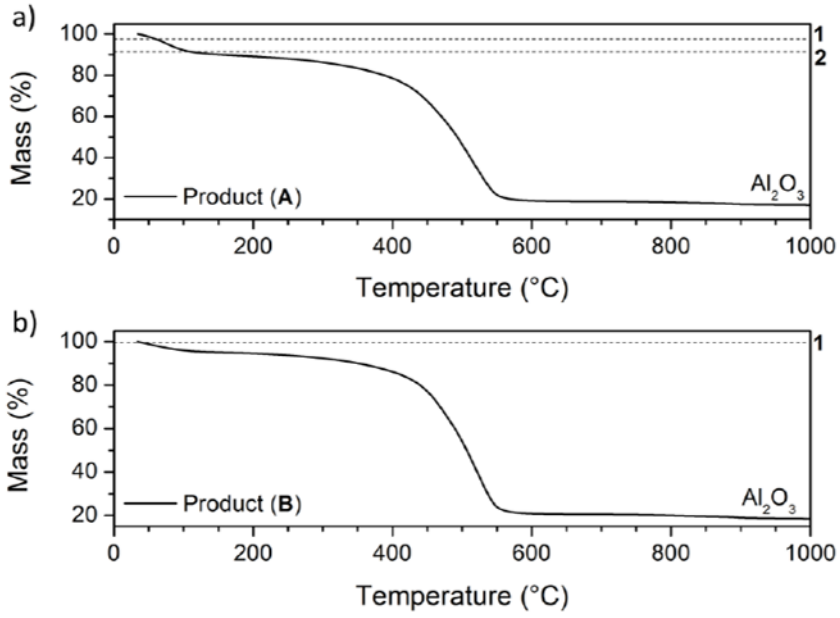

Figure 4: Thermogravimetric analysis (a) for Product **A** and (b) for Product **B.** The numerical labels 1 and 2 highlight the differences in first mass loss between the two materials.

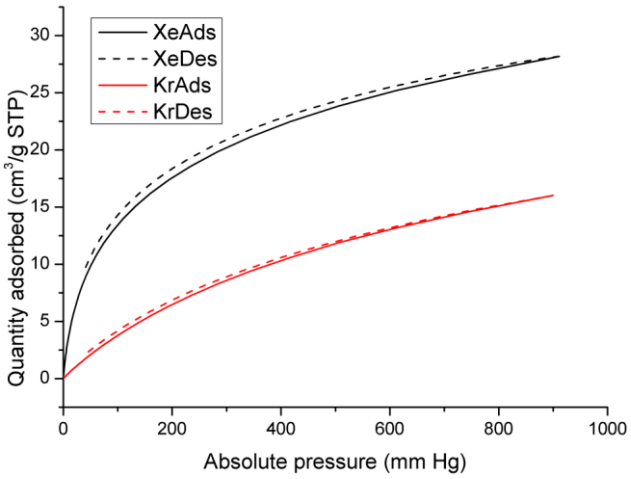

Figure 5: Isotherm curves (273.15 K) for the adsorption (solid) and the desorption (dash) of xenon (black) and krypton (red) in activated Product **B**.

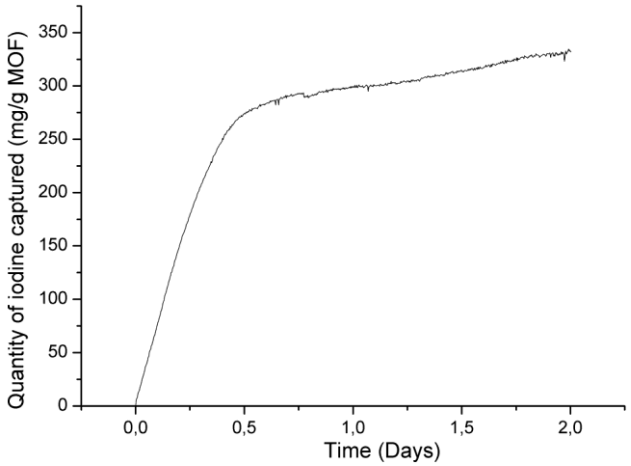

Figure 6: Iodine (I_2) adsorption curve for activated Product **B**.

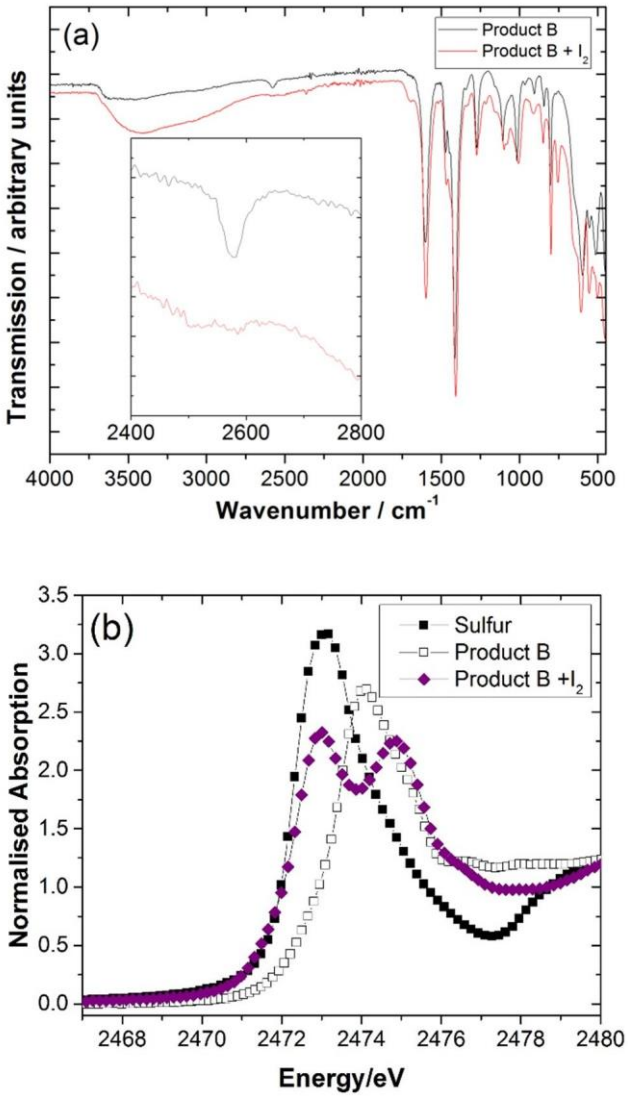

Figure 7: (a) IR spectra of thiol-modified MIL-53(Al)-SH_2 Product **B** before and after iodine exposure and (b) S K-edge XANES spectra before and after iodine adsorption (from solution).

References

[1] C. Serre, F. Millange, C. Thouvenot, M. Noguès, G. Marsolier, D. Louër and G. Férey, *J. Am. Chem. Soc.*, 2002, **124**, 13519-13526.

[2] G. Férey and C. Serre, *Chem. Soc. Rev.*, 2009, **38**, 1380-1399.

[3] R. I. Walton, A. S. Munn, N. Guillou and F. Millange, *Chem. Eur. J.*, 2011, **17**, 7069-7079; C. Nanthamathee, S. Ling, B. Slater and M. P. Attfield, *Chem. Mater.*, 2015, **27**, 85-95.

[4] F. Nouar, T. Devic, H. Chevreau, N. Guillou, E. Gibson, G. Clet, M. Daturi, A. Vimont, J. M. Grenèche, M. I. Breeze, R. I. Walton, P. L. Llewellyn and C. Serre, *Chem. Commun.*, 2012, **48**, 10237-10239; M. I. Breeze, G. Clet, B. C. Campo, A. Vimont, M. Daturi, J.-M. Grenèche, A. J. Dent, F. Millange and R. I. Walton, *Inorg. Chem.*, 2013, **52**, 8171-8182.

[5] T. Ahnfeldt, D. Gunzelmann, T. Loiseau, D. Hirsemann, J. Senker, G. Férey and N. Stock, *Inorg. Chem.*, 2009, **48**, 3057-3064; T. Devic, P. Horcajada, C. Serre, F. Salles, G. Maurin, B. Moulin, D. Heurtaux, G. Clet, A. Vimont, J. M. Greneche, B. Le Ouay, F. Moreau, E. Magnier, Y. Filinchuk, J. Marrot, J. C. Lavalley, M. Daturi and G. Férey, *J. Am. Chem. Soc.*, 2010, **132**, 1127-1136.

[6] S. Biswas, T. Ahnfeldt and N. Stock, *Inorg. Chem.*, 2011, **50**, 9518-9526.

[7] N. A. Ramsahye, T. K. Trung, S. Bourrelly, Q. Y. Yang, T. Devic, G. Maurin, P. Horcajada, P. L. Llewellyn, P. Yot, C. Serre, Y. Filinchuk, F. Fajula, G. Férey and P. Trens, *J. Phys. Chem. C*, 2011, **115**, 18683-18695; T. Devic, F. Salles, S. Bourrelly, B. Moulin, G. Maurin, P. Horcajada, C. Serre, A. Vimont, J.-C. Lavalley, H. Leclerc, G. Clet, M. Daturi, P. L. Llewellyn, Y. Filinchuk and G. Férey, *J. Mater. Chem.*, 2012, **22**, 10266-10273; N. Reimer, B. Gil, B. Marszalek and N. Stock, *CrystEngComm*, 2012, **14**, 4119-4125; P. Serra-Crespo, E. Gobechiya, E. V. Ramos-Fernandez, J. Juan-Alcaniz, A. Martinez-Joaristi, E. Stavitski, C. E. A. Kirschhock, J. A. Martens, F. Kapteijn and J. Gascon, *Langmuir*, 2012, **28**, 12916-12922; S. Biswas, S. Couck, D. Denysenko, A. Bhunia, M. Grzywa, J. F. M. Denayer, D. Volkmer, C. Janiak and P. Van Der Voort, *Micropor. Mesopor. Mater.*, 2013, **181**, 175-181; J. Wack, R. Siegel, T. Ahnfeldt, N. Stock, L. Mafra and J. Senker, *J. Phys. Chem. C*, 2013, **117**, 19991-20001.

[8] S. Biswas, T. Remy, S. Couck, D. Denysenko, G. Rampelberg, J. F. M. Denayer, D. Volkmer, C. Detavernier and P. Van Der Voort, *Phys. Chem. Chem. Phys.*, 2013, **15**, 3552-3561.

[9] A. S. Munn, R. S. Pillai, S. Biswas, N. Stock, G. Maurin and R. I. Walton, *Dalton Trans.*, 2016, **45**, 4162-4168.

[10] C. Volkringer and S. M. Cohen, *Angew. Chem., Int. Ed.*, 2010, **49**, 4644-4648; D. M. Zhang, Y. J. Guan, E. J. M. Hensen, T. Xue and Y. M. Wang, *Catal. Sci. Tech.*, 2014, **4**, 795-802; M. A. Gotthardt, R. Schoch, T. S. Brunner, M. Bauer and W. Kleist, *ChemPlusChem*, 2015, **80**, 188-195.

[11] K.-K. Yee, N. Reimer, J. Liu, S.-Y. Cheng, S.-M. Yiu, J. Weber, N. Stock and Z. Xu, *J. Am. Chem. Soc.*, 2013, **135**, 7795-7798.

[12] K.-K. Yee, Y.-L. Wong, M. Zha, R. Y. Adhikari, M. T. Tuominen, J. He and Z. Xu, *Chem. Commun.*, 2015, **51**, 10941-10944.

[13] B. Gui, K.-K. Yee, Y.-L. Wong, S.-M. Yiu, M. Zeller, C. Wang and Z. Xu, *Chem. Commun.*, 2015, **51**, 6917-6920.

[14] A. D. Burrows, C. G. Frost, M. F. Mahon and C. Richardson, *Chem. Commun.*, 2009, 4218-4220.

[15] G.-S. Yang, Z.-L. Lang, H.-Y. Zang, Y.-Q. Lan, W.-W. He, X.-L. Zhao, L.-K. Yan, X.-L. Wang and Z.-M. Su, *Chem. Commun.*, 2013, **49**, 1088-1090.

[16] J. He, K.-K. Yee, Z. Xu, M. Zeller, A. D. Hunter, S. S.-Y. Chui and C.-M. Che, *Chem. Mater.*, 2011, **23**, 2940-2947.

[17] X. P. Zhou, Z. T. Xu, M. Zeller and A. D. Hunter, *Chem. Commun.*, 2009, 5439-5441.

[18] X. P. Zhou, Z. T. Xu, J. He, M. Zeller, A. D. Hunter, R. Clerac, C. Mathoniere, S. S. Y. Chui and C. M. Che, *Inorg. Chem.*, 2010, **49**, 10191-10198.
[19] F. Ke, L.-G. Qiu, Y.-P. Yuan, F.-M. Peng, X. Jiang, A.-J. Xie, Y.-H. Shen and J.-F. Zhu, *J. Hazard. Mater.*, 2011, **196**, 36-43.
[20] T. Liu, J.-X. Che, Y.-Z. Hu, X.-W. Dong, X.-Y. Liu and C.-M. Che, *Chem. Eur. J.*, 2014, **20**, 14090-14095.
[21] X. Cheng, M. Liu, A. Zhang, S. Hu, C. Song, G. Zhang and X. Guo, *Nanoscale*, 2015, **7**, 9738-9745.
[22] F. C. Kuepper, M. C. Feiters, B. Olofsson, T. Kaiho, S. Yanagida, M. B. Zimmermann, L. J. Carpenter, G. W. Luther, III, Z. Lu, M. Jonsson and L. Kloo, *Angew. Chem., Int. Ed.*, 2011, **50**, 11598-11620.
[23] L. Vial, R. F. Ludlow, J. Leclaire, R. Perez-Fernandez and S. Otto, *J. Am. Chem. Soc.*, 2006, **128**, 10253-10257.
[24] Topas V4.2: General Profile and Structure Analysis Software for Powder Diffraction Data, Bruker AXS Ltd, 2008.
[25] B. Ravel and M. Newville, *J. Synchrotron Rad.*, 2005, **12**, 537-541.
[26] A. Vairavamurthy, *Spectrochim. Acta. Part A*, 1998, **54**, 2009-2017.
[27] T. Loiseau, C. Serre, C. Huguenard, G. Fink, F. Taulelle, M. Henry, T. Bataille and G. Férey, *Chem. Eur. J.*, 2004, **10**, 1373-1382.
[28] A. Boutin, M. A. Springuel-Huet, A. Nossov, A. Gédéon, T. Loiseau, C. Volkringer, G. Férey, F. X. Coudert and A. H. Fuchs, *Angew. Chem., Int. Ed.*, 2009, **48**, 8314-8317.
[29] D. Banerjee, A. J. Cairns, J. Liu, R. K. Motkuri, S. K. Nune, C. A. Fernandez, R. Krishna, D. M. Strachan and P. K. Thallapally, *Acc. Chem. Res.*, 2015, **48**, 211-219.
[30] C. Falaise, C. Volkringer, J. Facqueur, T. Bousquet, L. Gasnot and T. Loiseau, *Chem. Commun.*, 2013, **49**, 10320-10322.
[31] S. L. Ma, S. M. Islam, Y. Shim, Q. Y. Gu, P. L. Wang, H. Li, G. B. Sun, X. J. Yang and M. G. Kanatzidis, *Chem. Mater.*, 2014, **26**, 7114-7123.
[32] K. S. Subrahmanyam, D. Sarma, C. D. Malliakas, K. Polychronopoulou, B. J. Riley, D. A. Pierce, J. Chun and M. G. Kanatzidis, *Chem. Mater.*, 2015, **27**, 2619-2626.
[33] K. K. Yee, Y. L. Wong and Z. T. Xu, *Dalton Trans.*, 2016, **45**, 5334-5338.